

Date of publication xxxx 00, 0000, date of current version xxxx 00, 0000.

Digital Object Identifier

# Empirical Comparison of Four Stereoscopic Depth Sensing Cameras for Robotics Applications

LUKAS RUSTLER<sup>1,\*</sup>, VOJTECH VOLPRECHT<sup>1,\*</sup>, and MATEJ HOFFMANN<sup>1</sup>

<sup>1</sup>Department of Cybernetics, Faculty of Electrical Engineering, Czech Technical University in Prague

\*The authors contributed equally

Corresponding author: Matej Hoffmann (e-mail: matej.hoffmann@fel.cvut.cz).

This work was co-funded by the European Union under the project Robotics and Advanced Industrial Production (reg. no. CZ.02.01.01/00/22\_008/0004590). L.R. was additionally supported by the Grant Agency of the Czech Technical University in Prague, grant No. SGS24/096/OHK3/2T/13.

**ABSTRACT** Depth sensing is an essential technology in robotics and many other fields. Many depth sensing (or RGB-D) cameras are available on the market and selecting the best one for your application can be challenging. In this work, we tested four stereoscopic RGB-D cameras that sense the distance by using two images from slightly different views. We empirically compared four cameras (Intel RealSense D435, Intel RealSense D455, StereoLabs ZED 2, and Luxonis OAK-D Pro) in three scenarios: (i) planar surface perception, (ii) plastic doll perception, (iii) household object perception (YCB dataset). We recorded and evaluated more than 3,000 RGB-D frames for each camera. For table-top robotics scenarios with distance to objects up to one meter, the best performance is provided by the D435 camera. For longer distances, the other three models perform better, making them more suitable for some mobile robotics applications. OAK-D Pro additionally offers integrated AI modules (e.g., object and human keypoint detection). ZED 2 is not a standalone device and requires a computer with a GPU for depth data acquisition. All data (more than 12,000 RGB-D frames) are publicly available at <https://osf.io/f2seb>.

**INDEX TERMS** Depth Sensing, Intel RealSense, Luxonis OAK-D Pro, ZED 2, Object Detection, RGB-D, Segmentation

## I. INTRODUCTION

DEPTH sensing cameras, or RGB-D cameras, are visual sensors providing standard images (RGB), along with depth information. They are compact, powerful, and affordable sensors, making them attractive for a wide range of applications in robotics and many other fields. In this work, we compare four different RGB-D cameras: Intel RealSense D435 [1], Intel RealSense D455 [2], StereoLabs ZED 2 [3], and Luxonis OAK-D Pro [4]. All of the cameras work on the stereoscopic principle—the actual physical sensor contains two cameras with a fixed distance and the depth is computed from matching features in the two streams. RealSense and OAK-D Pro devices are active, i.e., they project an IR grid that helps with feature matching. Depth can be also perceived using Time-of-Flight (ToF) sensors, like LIDAR, which perceive depth more accurately, but are more bulky and expensive. They are typically used on large mobile robots and are not deployed in indoor robot manipulation [5].

The accuracy of the sensors is crucial for the correct use and deployment. However, manufacturers usually provide only technical specifications and information on the percentual

accuracy in a given depth [1]–[4]. This information is useful, but it is not informative about the standard deviation in individual underlying tasks and was usually measured under unknown laboratory conditions that are hard to replicate in daily use. Researchers always wanted to better estimate the camera capabilities in computer vision applications, as done by Andersen *et al.* [6] with the Kinect or Nguyen *et al.* [7] who tried to estimate the noise of the Kinect to improve its performance in Simultaneous Localization and Mapping (SLAM). After Kinect, Intel cameras became popular. Carfagni *et al.* provided a performance evaluation of Intel RS300 [8]. Some researchers also compared stereo vision cameras with ToF cameras [9] or only ToF [10]. Tadic *et al.* performed comparison of Intel and StereoLabs cameras from the point-of-view of technical specifications and from visual inspection of depth images [11]. Other ZED camera analysis was performed in [12], where the authors tested the camera in indoor environments. Halmetschlager *et al.* [13] compared 10 depth-sensing cameras with different working principles, proposed a noise model, and advised which camera to use for which purpose.

Some works focused more on accuracy in a given task,

arXiv:2501.07421v1 [cs.RO] 13 Jan 2025

e.g., bolt tightening [14] or fruit detection and sizing [15], [16]. More unusual research containing RGB-D cameras can be the comparison with multi-view stereo for face surface reconstruction [17] or learning how to recognize a camera model or light source only from depth noise [18]. Similar comparisons to ours were made by Heinemann *et al.* [19] who compared six cameras, including the ones we have, in bias and standard deviation on flat surfaces, spheres and one 3D box. Other recent and comparable study was proposed by Servi *et al.* [20]. The authors compared 4 cameras (not the same set as us) using planes, spheres, and a 3D printed statue.

**Contribution.** The unique contribution of this work is an extensive experimental evaluation of four state-of-the-art RGB-D cameras on object perception. While previous works have mostly assessed performance on planar surfaces, we additionally evaluate performance on a plastic doll figure and on a standard robotics benchmark object dataset (YCB). Furthermore, we have employed five different evaluation metrics, including those used in 3D object reconstruction (Chamfer Distance and Jaccard Similarity). Our conclusions are thus directly relevant to the object perception and robot manipulation community. We provide an overview of the cameras' technical parameters as well as their user interfaces. Finally, we make our dataset with more than 12,000 segmented RGB-D images publicly available for the community. This dataset can serve not only to estimate the camera precision, but also as ground truth for RGB-D segmentation or object perception pipelines.

## II. CAMERAS AND SPECIFICATIONS

This section describes the hardware used and its technical specifications. The RGB-D cameras used in this work can be seen in Fig. 1 and their main technical specifications can be found in Table 1. All four cameras use the stereoscopic effect to compute the depth. In other words, the depth is computed from correspondences in two images from slightly different views. Both RealSense devices and the OAK-D Pro camera use active stereo, i.e., they project additional IR points that help to find correspondences.



**FIGURE 1.** RGB-D cameras used in the experiments. The cameras are shown in scale—width of D435 camera in a) is 90 mm.

**On-board computation.** The Intel cameras (D435, D455) perform depth computation on-board, and resources of a host computer are used only for potential post-processing. ZED 2, on the other hand, requires the host computer to contain CUDA-enabled Graphical Processing Unit (GPU) to compute the depth. The benefit arising from GPU necessity is that StereoLabs provides a wide selection of Artificial Intelligence

(AI) tools, such as object detection or body tracking, which can be run through their Application Programming Interface (API) directly using the camera output. The OAK-D Pro camera performs all computations on board, but still provides AI features that also run directly on the camera.

**Depth accuracy.** In terms of depth accuracy reported by the respective manufacturers, D455, ZED 2, and OAK-D Pro should perform similarly with an error of  $< 2\%$  at 4 m. The D435 should, according to the specifications, be twice less accurate with error of  $< 2\%$  at 2 m. The devices that do not require GPU (D435, D455, OAK-D Pro) have similar maximal depth resolution (1280x720). However, the Frames per Second (FPS) with the maximal resolution is 30 for D435, D455 and 120 for OAK-D Pro. RealSense devices can get up to 90, but the resolution needs to be lower. These three cameras also have a similar Field of View (FOV). For ZED 2, the maximum resolution can be up to 2K with 15FPS (ZED 2 can get up to 100FPS based on the resolution) with larger FOV.

**Dimensions and range.** The cameras also differ in their dimensions. D435 and OAK-D Pro are both quite small (less than 10 cm in length), D455 is longer, and ZED 2 is the longest, with almost twice the length as for D435. The physical dimension results in a different stereo baseline and influences the range of the sensor. The ideal range for 435 is [0.3 m, 3 m], whereas its [0.6 m, 6 m] for D455, [0.8 m, 12 m] for OAK-D Pro (this is an exception, as the range is enhanced with custom processing) and [0.3 m, 20 m] for ZED 2. However, the D435 with the shortest stereo baseline and limited maximum range is, on the other hand, best suited for depth perception close to the camera.

**Price.** RealSense D435 costs 314\$, Luxonis OAK-D Pro 349\$, RealSense D455 419\$ and StereoLabs ZED2 449\$. Prices are from the respective official websites at the time of writing this article.

## III. SETUP AND EVALUATION

The setup utilized to record the experiments is depicted in Fig. 2. We mounted the four cameras on tripods in a long hallway and set the tripods so that the sensors of the individual sensors were at the same height and level. In front of the cameras, there is a table. We always moved the table or objects on top of the table, not the cameras. We tested three scenarios: (i) planar surface perception, where only the planar surface behind the doll in Fig. 2 was recorded; (ii) plastic doll perception, where a doll was captured by the cameras (corresponds to Fig. 2); (iii) and YCB objects perception, where objects from the YCB Object and Model set [21] <https://www.ycbbenchmarks.com/> were perceived (without the planar surface behind). The scenarios were selected to compare the cameras in terms of flat surface sensing (planes) and on more complicated objects (doll, YCB) as it is an important task for underlying robotic tasks such as segmentation, perception, or grasping.

The cameras were connected to one computer with a NVIDIA RTX 3070 GPU and Intel Core i9-11900 CPU.

**TABLE 1.** Technical parameters of the cameras used in this study. \*Stated by the manufacturers. \*\*Not with maximal resolution.

Camera	Stereo Technology	Ideal Range [m]	Depth				RGB			Dimensions [mm]	GPU	AI
			Accuracy*	FOV	Max Resolution	Max FPS	FOV	Max Resolution	Max FPS			
D435	Active	0.3 - 3	<2% at 2 m	87° × 58°	1280x720	90**	69° × 42°	1920x1080	30	90x25x25	×	×
D455	Active	0.6 - 6	<2% at 4 m	87° × 58°	1280x720	90**	90° × 65°	1280x800	30	124x26x29	×	×
ZED 2	Passive	0.3 - 20	<0.8% at 2 m	110° × 70°	2208x1242	100**	110° × 70°	2208x1242	100**	175x30x32	✓	✓
OAK-D Pro	Active	0.8 - 12	<2% at 4 m	80° × 55°	1280x800	120	66° × 54°	4056x3040	60	97x23x30	×	✓

**FIGURE 2.** Experimental setup illustration – plastic doll perception.

To eliminate the computational processing requirements, we always recorded output from one camera at a time. RealSense cameras were recorded through the RealSense Viewer application. ZED 2 and OAK-D Pro through their respective Python API. We used default settings for each camera—see Table 2. No post-processing was applied.

**TABLE 2.** Camera settings used in the experiments. \*Name in the corresponding API. All are default for the given camera.

Camera	Depth Resolution	FPS	Mode*
D435	848x480	30	Default
D455	848x480	30	Default
ZED 2	1920x1080	30	ULTRA
OAK-D Pro	1280x800	30	HIGH_ACCURACY

### A. DATA ACQUISITION AND PROCESSING

In all scenarios, we always recorded the static scene for at least two seconds with every camera. However, the scenarios require different data processing for proper evaluation.

- Planes – In this case, we only moved the table further away from the cameras to different distances. Then, from the resulting point cloud, we extracted a square with a side of 10 cm with a center in front of the camera.
- Plastic doll and YCB objects – In this case, we moved the table further away and also moved the individual objects so that they are in front of the respective camera all the time. Then, from the resulting point clouds, we segmented the object. The segmentation was partially automatic (plane extraction, depth cropping) and partially manual to properly segment only the object of interest.

To evaluate the results, we needed to fit the segmented point clouds to a ground truth. We utilized the Iterative Closest Point (ICP) [22] algorithm for an initial transformation. Further, we manually checked every estimated transformation and refined it to fit the ground truth properly. We used more than one frame for each object (for each camera at every depth), but we used only one transformation for the given setting. Otherwise, ICP could change the accuracy results, as it could mitigate the error by a transformation.

### B. GROUND-TRUTH POINT CLOUDS

For some metrics, ground-truth point clouds (shapes) are needed. For planar surfaces, we simply created a point cloud of a square with a side of 10 cm. For the doll, there is no ground truth available. We utilized photogrammetry to create the model of the doll, i.e., we took a number of pictures of the doll from various angles and used Meshroom [23] to create a point cloud of the doll. The YCB dataset was selected because it provides real-world items with corresponding models of the objects. Thus, for objects from YCB we downloaded the corresponding model and sampled them into point clouds. For the transparent spray bottle, ground truth is not available from YCB, so we used photogrammetry like in the case of the plastic doll.

The ground truth point clouds for the YCB objects are complete point clouds from all sides. However, in our experiments, we obtained point clouds from one view only. To make comparison fair, we manually cropped the ground-truth point clouds to match the viewpoint of the depth cameras.

### C. EVALUATION AND METRICS

We selected a set of metrics that compare different aspects of performance in all scenarios. Not all of them can be used in all scenarios. The definitions of the metrics are given below.

### 1) Bias and Standard Deviation

This metric is also used in [13], [19]. Bias describes the error between the mean estimated distance by the sensors and the ground-truth distance. It is defined as

$$\text{bias} = |d_{gt} - \mu|, \quad (1)$$

where  $d_{gt}$  is the ground-truth distance and  $\mu$  is the mean distance from the sensor defined as

$$\mu = \frac{1}{N \cdot M} \sum_{i=1}^N \sum_{j=1}^M d_{i,j}, \quad (2)$$

where  $N$  is number of frames,  $M$  is number of points in the given frame and  $d_{i,j}$  is depth at point  $j$  of frame  $i$ .

The standard deviation (SD) of depth measurements is defined as

$$SD = \sqrt{\frac{1}{N \cdot M} \sum_{i=1}^N \sum_{j=1}^M (d_{i,j} - \mu)^2}, \quad (3)$$

where  $\mu$  is from (2).

This metric is used only for planar surface perception.

### 2) Chamfer Distance

Chamfer Distance (CD) is a standard metric for estimating the distance of two point clouds. It is defined as the average distance of each point in one set to the closest point in the second set and vice versa, i.e.,

$$d_{CD}(\mathbf{S}_1, \mathbf{S}_2) = \frac{1}{N} \sum_{\mathbf{x} \in \mathbf{S}_1} \min_{\mathbf{y} \in \mathbf{S}_2} \|\mathbf{x} - \mathbf{y}\|_2 + \quad (4)$$

$$\frac{1}{M} \sum_{\mathbf{y} \in \mathbf{S}_2} \min_{\mathbf{x} \in \mathbf{S}_1} \|\mathbf{x} - \mathbf{y}\|_2, \quad (5)$$

where  $N, M$  are number of elements in  $\mathbf{S}_1$  and  $\mathbf{S}_2$ , respectively. In this case,  $\mathbf{S}_1$  and  $\mathbf{S}_2$  are segmented point clouds from the camera and ground-truth point clouds, respectively. This metric is used for plastic doll and YCB objects perception.

### 3) Jaccard Similarity

Jaccard Similarity (JS) is a standard metric for estimating the geometric similarity of two shapes—with values from 0 to 1. It is defined as intersection over union of voxelized shapes, i.e.,

$$J(\mathbf{S}_1, \mathbf{S}_2) = \frac{|\mathbf{S}_1 \cap \mathbf{S}_2|}{|\mathbf{S}_1 \cup \mathbf{S}_2|}, \quad (6)$$

where  $\mathbf{S}_1, \mathbf{S}_2$  are two sets. In our case,  $\mathbf{S}_1$  and  $\mathbf{S}_2$  are segmented and voxelized point clouds from the camera and ground-truth point clouds, respectively.

This metric is used for plastic doll and YCB objects perception. The higher the value, the better.

### 4) F-score

$F_1$  score is a harmonic mean of the precision and recall measures used in classification—with values from 0 to 1. We used the definition from NVIDIA Kaolin Library [24], where True Positive (TP) is defined by the existence of two points in a given radius  $r$  from each other. False Negative (FN) are points in the camera point cloud that are further than  $r$  from the closest point in ground truth and False Positive (FP) are points from the ground truth that are further than  $r$  from the camera point cloud. And then

$$F_1 = \frac{2TP}{2TP + FP + FN}. \quad (7)$$

This metric is used for YCB objects and plastic doll perception. The higher the value, the better.

### 5) Angle between Normals

This metric shows the angle between normals of two closest points in estimated and ground-truth point clouds. For each point in the camera point cloud, we find the closest point in the ground-truth point cloud and compute the angle as

$$\theta = \arccos \frac{n_1 \cdot n_2}{|n_1| \cdot |n_2|}, \quad (8)$$

where  $n_1, n_2$  are normals of two closest points.

An example is shown in Fig. 3, where blue lines show normals of the ground-truth point cloud and red lines show normals of the captured point cloud.

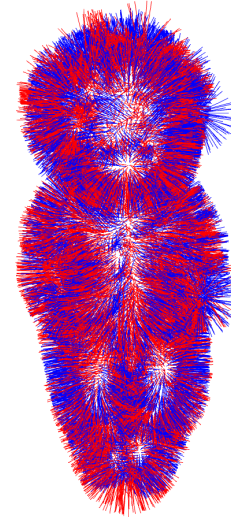


**FIGURE 3.** Normals of the ground-truth (blue) and captured (red) point cloud of the plastic doll.

This metric is used for all scenarios.

## IV. EXPERIMENTS AND RESULTS

We tested the four cameras in three different scenarios: (i) planar surface perception, (ii) plastic doll perception, (iii) YCB objects perception. We measured each of these at several distances. For every object experiment, we used 30 successive frames, converted them to point clouds, and segmented the



object out of the frame. Distances from the camera to the objects were measured with a laser measuring device and data were captured under constant light conditions of about 420 lx. In total, we compared the cameras with more than 3,000 point clouds from each camera, resulting in more than 12,000 total point clouds. All segmented point clouds, together with depth and RGB images, can be found at <https://osf.io/f2seb>.

### A. PLANAR SURFACE PERCEPTION

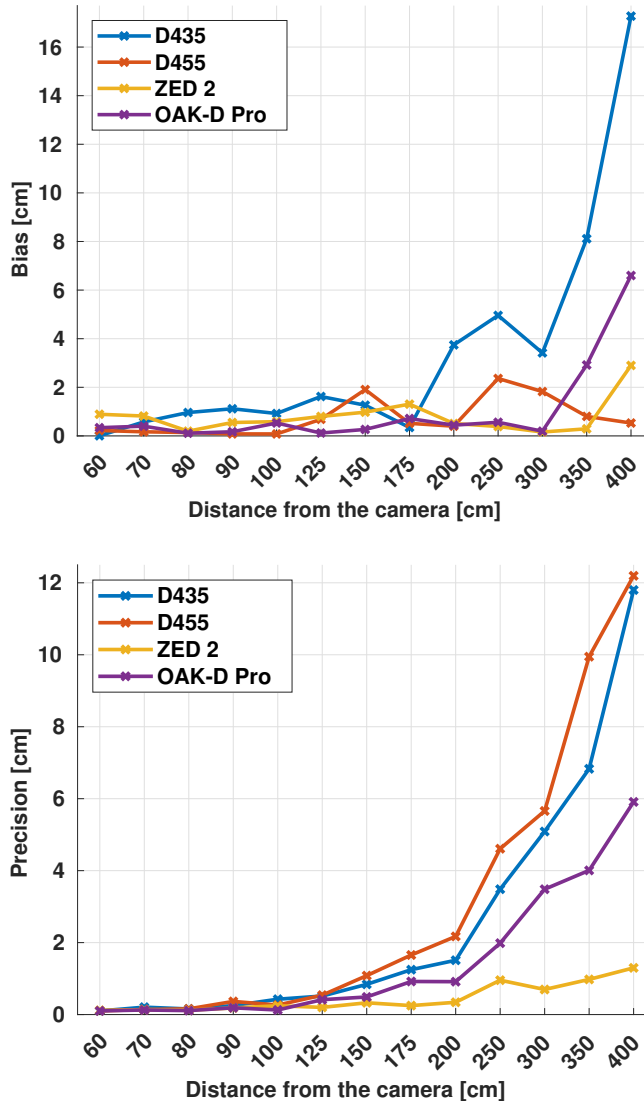


**FIGURE 4.** Planar surface perception – bias and standard deviation. The values for each distance and camera are averaged from 30 frames. (Top) Bias in distance estimation to the plane (0 bias is correct). (Bottom) – Standard deviation of the estimates.

We recorded samples at 60, 70, 80, 90, 100, 125, 150, 175, 200, 250, 300, 350, and 400 cm from the camera. Fig. 4 shows the bias and standard deviation (defined in Section III-C1) for  $10 \times 10$  cm squares extracted from 30 consecutive frames taken by the cameras. For all cameras, the bias (error of the mean distance) is small ( $<2$  cm) up to 175 cm. Then, the

bias of D435 increases significantly, mainly beyond 300 cm, corresponding to the max. range of the D435. The OAK-D Pro bias starts to deviate after 300 cm. For ZED 2 and D455, the bias is  $<3$  cm even at the farthest distance.

For standard deviation of distance from 30 measurements, all cameras behave similarly up to 100 cm with error  $<0.5$  cm. Then, the RealSense devices (D435, D455) start to lose precision; this is also the case for the OAK-D Pro but to a lesser extent. In case of ZED 2, the standard deviation is  $<1.5$  cm for all distances.

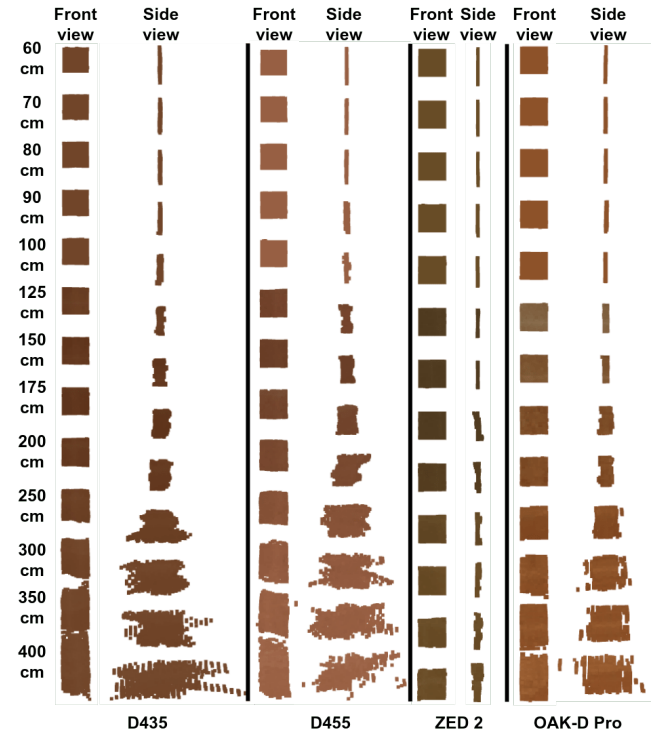


**FIGURE 5.** Planar surface perception – point clouds. Front (left columns) and side (right columns) views on point clouds of the extracted planes (concatenated over all 30 frames) for all distances.

The standard deviation can also be seen in the right columns of Fig. 5, where it is represented as the scatter of the points on the sides. It is well visible that, except for ZED 2, the width of the planes is getting bigger with increasing distance, corresponding to a increase in standard deviation in Fig. 4.

Another metric usable for planes perception is the angle between the closest normals in camera and ground-truth point clouds. In case of planes, this metric is basically a metric of flatness. The results can be seen in Fig. 6. Up to 80 cm all cameras stay under  $0.2$  rad ( $\sim 10^\circ$ ). However, the RealSense devices have twice the error even at the lower distances. At higher distances, the error of the RealSense devices increases to around  $1$  rad ( $\sim 60^\circ$ ). ZED 2 stays  $<0.2$  rad and OAK-D Pro  $<0.1$  rad for all distances. Farther than 100 cm from the camera, The RealSense devices (D435, D455) have more variability over different frames, while OAK-D Pro and ZED 2 show only small variability. The planes extracted from D435

and D455 are more uneven with increasing distance. The planes extracted from ZED 2 and OAK-D Pro are equally flat for all distances. OAK-D Pro, in fact, always returns points in almost “flat layers”, and thus the error from a flat surface is low.

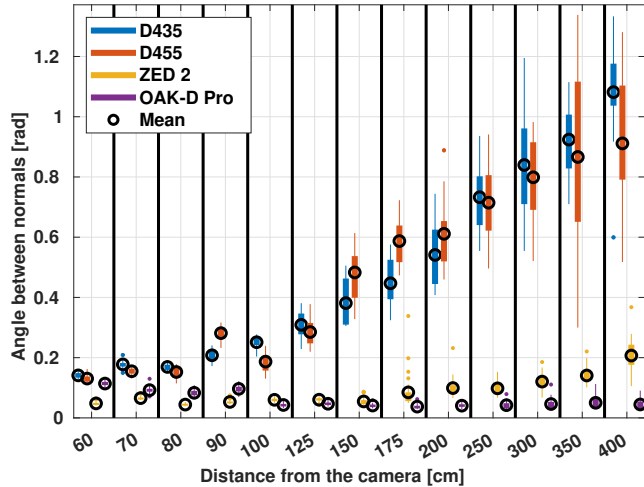


**FIGURE 6.** Planar surface perception – angles between the closest normals. Bars show values from 25th to 75th percentile; whiskers represent non-outlier extreme points and dots represent outliers. Computed over 30 frames for each distance and camera. The lower the value, the better.

**Planar surface perception – summary.** All the results, Fig. 4, Fig. 5, Fig. 6 paint a coherent picture. For distances above one meter, D435 and D455 start losing both accuracy (positive bias – distance overestimation) and precision (greater variability). ZED 2 has very good performance even for the maximum tested distance (400 cm).

**B. PLASTIC DOLL PERCEPTION**

The second set of experiments involved perception of a plastic doll shown in Fig. 2. We recorded the samples at 90, 100, 125, 150, 175, 200, 250, 300, 350, and 400 cm from the camera. Point clouds taken from 125 cm and 400 cm can be seen in Fig. 7. We can see that at the closer distance, the point clouds look visually fine from both front and side views. The most visible flaws are at the forehead, which is a challenging part for RGB-D cameras as it is featureless and shiny. On the other hand, in the farther distance the point clouds are much noisier. The noise is visible especially from the side view, where the uneven depth estimation is visible for all cameras. However, it is interesting how different cameras handle the depth differently. RealSense devices divide the depth into layers with small differences between them and include some noisy points. OAK-D Pro divides the distances into layers with higher distances without visible noise. ZED 2 has the lowest depth difference among individual frames, but has the most noisy points.

The first empirical metric we can look at is the CD shown in Fig. 8. Note that at 90 and 100 cm, the OAK-D Pro camera did

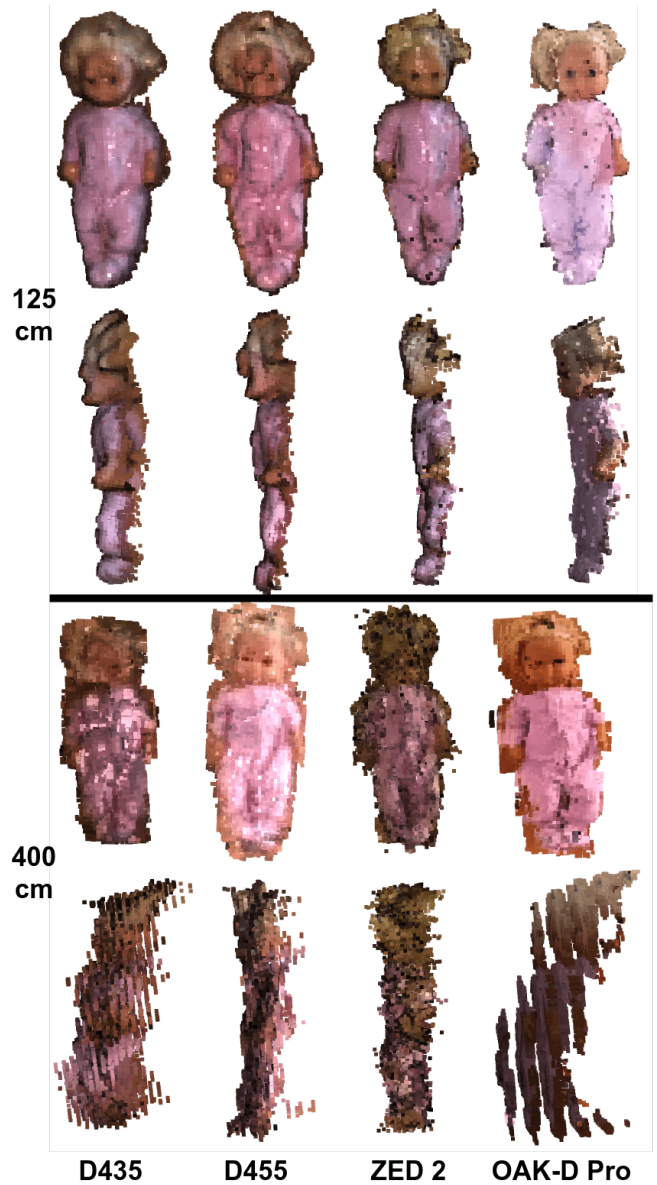


**FIGURE 7.** Plastic doll perception – point clouds. At 125 cm (upper block) and 400 cm (lower block) distance. Front and side views on the point clouds (concatenated over all 30 frames).

not see the entire doll, thus the comparison at these distances is not fair. Otherwise, until 175 cm all cameras stay under 2 cm error, with ZED 2 having the best performance, followed by D435. Interestingly, D455 behaves worse than D435. We assume that it is caused by a higher baseline of D455, which helps for flat surfaces but has a negative effect for more complicated surfaces. The error rises steeply after that for all cameras except ZED 2. At 400 cm ZED 2 still keeps the CD under 3 cm, whereas OAK-D Pro has more than 8 cm error. It is caused mainly by the layering of depth—visible in Fig. 7. At the final distance, D455 is finally better than D435, but, as has been said, this distance is above the ideal range of D435. The variance between individual frames is gradually increasing for all cameras except for ZED 2.

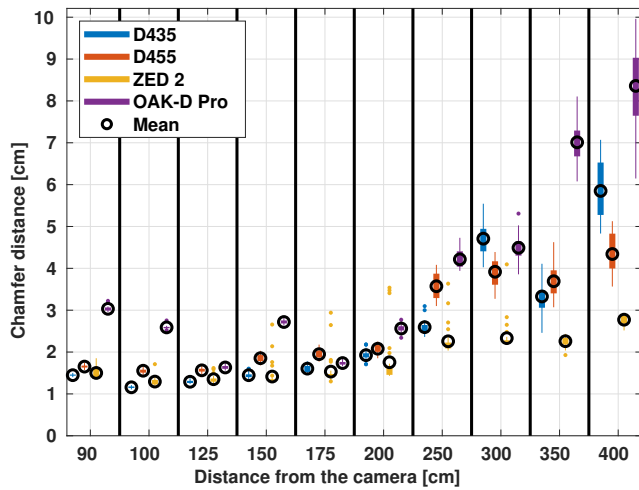


**FIGURE 8.** Plastic doll perception – Chamfer Distance (CD). Bars show values from 25th to 75th percentile; whiskers represent non-outlier extreme points and dots represent outliers. Computed over 30 frames for each distance and camera. The lower the value, the better.

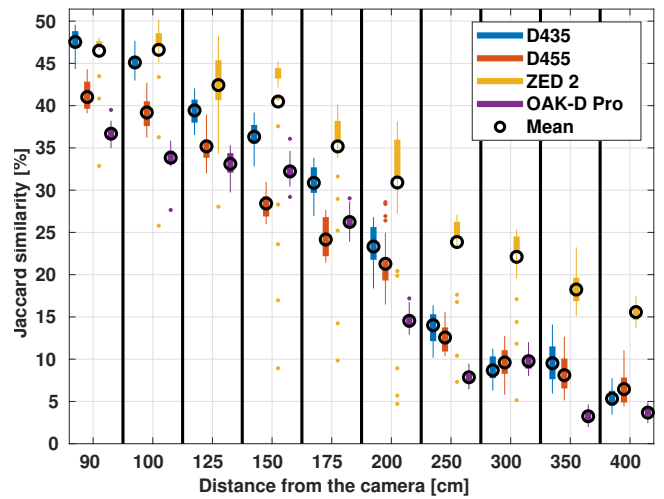


**FIGURE 10.** Plastic doll perception – Jaccard Similarity (JS). Bars show values from 25th to 75th percentile, whiskers represent non-outlier extreme points and dots represent outliers. Computed over 30 frames for each distance and camera. The higher the value, the better.

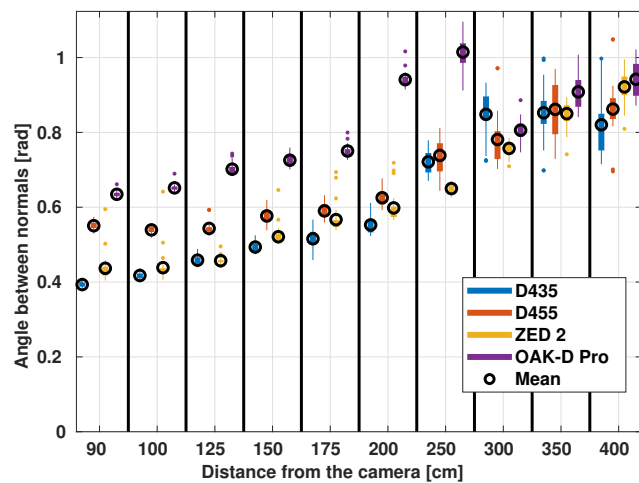


**FIGURE 9.** Plastic doll perception – angles between the closest normals. Bars show values from 25th to 75th percentile, whiskers represent non-outlier extreme points, and dots represent outliers. Computed over 30 frames for each distance and camera. The lower the value, the better.

The other metric is the angle between normals. Here, it is not a measure of flatness as in the case of planar surfaces, but rather a measure of shape estimation. The results can be seen in Fig. 9. An important thing to notice is the high error of the OAK-D Pro camera at all depths. As has been said, OAK-D Pro creates layers of points at different depths (the depth differences between layers are lower for a lower object distance from the camera) instead of a scatter distribution, as is for other cameras. That results in facing of the normals more in the direction of the camera plane. Among the other cameras, ZED 2 and D435 are on par for every distance and D455 is worse up to 150 cm (again, we attribute this to the wider baseline), and then all cameras perform almost

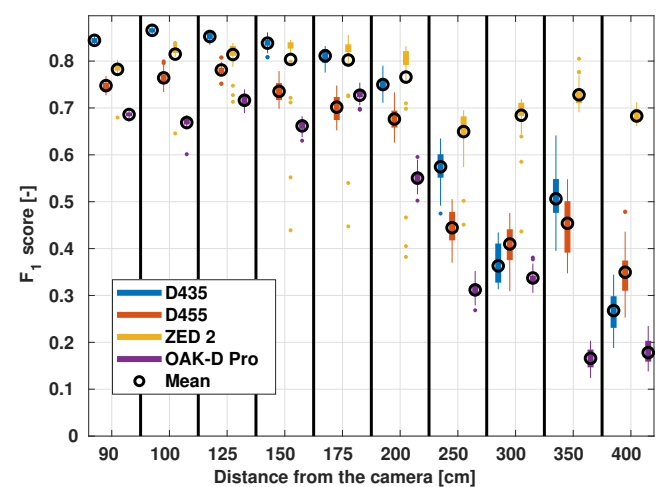


**FIGURE 11.** Plastic doll perception –  $F_1$  score. Bars show values from 25th to 75th percentile, whiskers represent non-outlier extreme points and dots represent outliers. Computed over 30 frames for each distance and camera. The higher the value, the better.

the same. Overall, the angles are higher than for the planar surfaces in lower distances—around 0.2 rad vs. 0.4 rad at the closest distance. However, it is interesting to look at the higher distances. RealSense devices achieve the same error as for the planes—about 1 rad. Both ZED 2 and OAK-D Pro are on par with Intel devices, but in the case of planes the error for the highest distance was under 0.2 rad for ZED 2 and 0.1 rad for OAK-D Pro. That is a huge difference that shows how the devices sense simple (planar) and more complex environments differently.

For the final two metrics—Jaccard Similarity (JS) and  $F_1$  score—the higher the value, the better. Both of these metrics evaluate the similarity of the shapes. In case of JS, the output

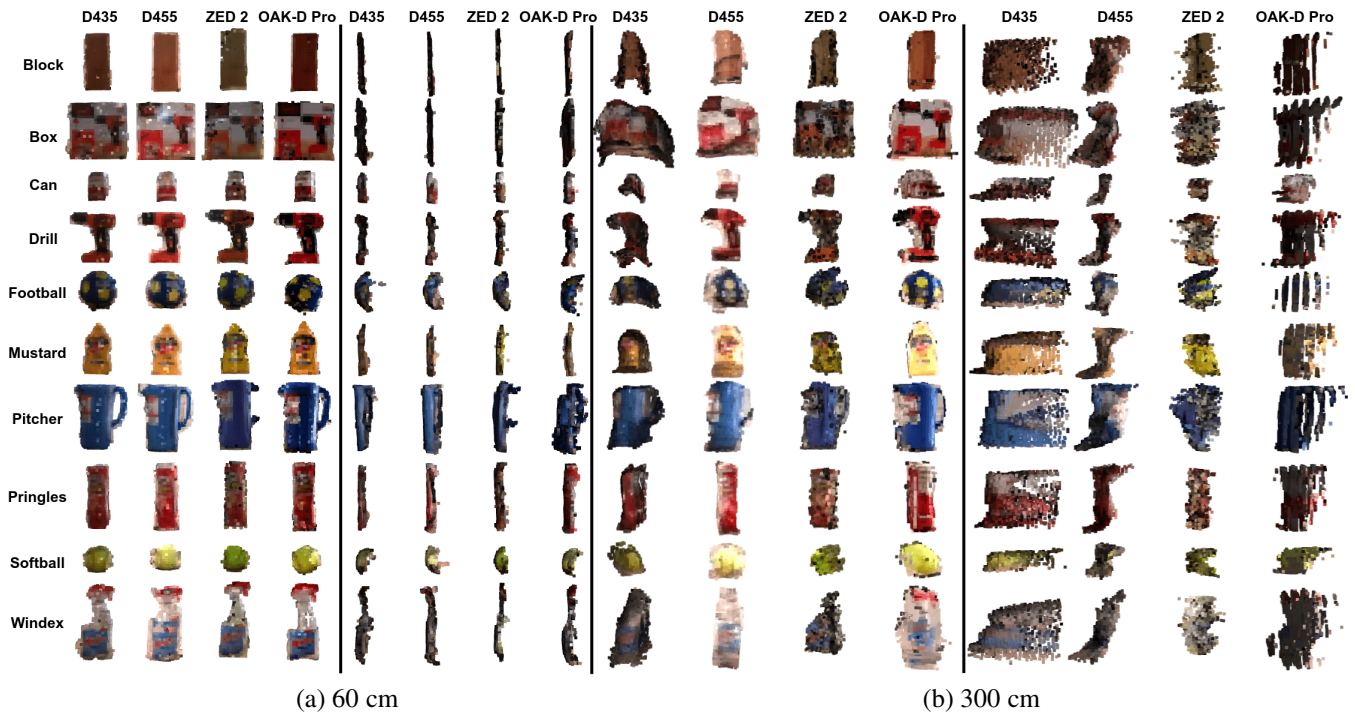


**FIGURE 12.** YCB objects perception – point clouds. Front (left blocks) and side (right blocks) views for 60 cm (a) and 300 cm (b).

is “geometric closeness” of two shapes. For  $F_1$ , it is the probability that a point in a given point cloud should be where it is when considering the ground truth. For D435, D455, and OAK-D Pro, the results are similar, with D435 being the best among those. In case of JS, the similarity is getting lower with a steeper drop from 250 cm further.  $F_1$  similarity also demonstrates the same drop. For ZED 2, JS is getting gradually lower without any significant drop, and  $F_1$  reveals only a slight drop (around 0.1) at higher distances. The reason is the amount of noise. As can be seen in the bottom block of Fig. 7, the ZED 2 point clouds have the lowest variance in depth estimates between frames, and the noise is more concentrated around the true values, compared to other cameras that produce more scattered results.

**Plastic doll perception – summary.** All the cameras performs similarly well up to 150 cm in all metrics. The best overall cameras is the ZED 2, that achieves CD error  $< 3$  cm even at the farthest distance (400 cm). The worst camera in this task is the OAK-D Pro. Both Intel devices perform similarly and up to 200 cm they are comparable to ZED 2 camera.

### C. YCB OBJECTS PERCEPTION

For this setting, we recorded at 60, 80, 100, 125, 150, 200, 250, and 300 cm from the cameras, where we used 10 different objects—see Fig. 12. The objects were selected to represent various shapes, sizes, and materials.

Fig. 12 includes front and side views of point clouds captured by the cameras at 60 cm and 300 cm. We can see that for the small distance, most of the objects are visually fine.

Some flaws can be seen for *can* and *windex bottle*. The main difference between the cameras is for the *pitcher*, where the best results come from D435 and OAK-D Pro. D455 was unable to detect the hole in the handle, and ZED 2 missed half of the handle. The side views are worse again for the *pitcher* and then for the *windex bottle*. The bottle is transparent, which is an adversarial surface for RGB-D cameras. At 300 cm, the best front views are generally distorted and noisy and the best are probably for D455 and ZED 2. The more interesting is the side view, which reveals a higher standard deviation in the depth estimation from D435 and OAK-D Pro. Point clouds for D455 and ZED 2 have less scatter in depth estimation, but ZED 2 has noisy points and D455 creates surface coplanar with the table at the bottom parts of the objects.

Chamfer Distance (CD) for the YCB objects can be seen in Fig. 13. We can see that the trend is the same as in the case in the plastic doll perception. Up to 150 cm all the cameras perform almost the same with CD around 1 cm. After that, the error for RealSense devices increases up to about 5.5 cm for D435. The best is ZED 2 with about 2 cm even at 300 cm. The difference from the plastic doll perception is that OAK-D Pro is now the second best camera in terms of mean CD. We assume that the reason is that some of the objects selected are flat, and thus OAK-D Pro performs well on these. But, as seen from a high variance and outlier points, it performs the worst on some objects.

Angles between the closest normals for YCB objects are shown in Fig. 14. The results are similar to the angles for the plastic doll perception (see Fig. 9), with the difference for OAK-D Pro. In case of the plastic doll perception, there was



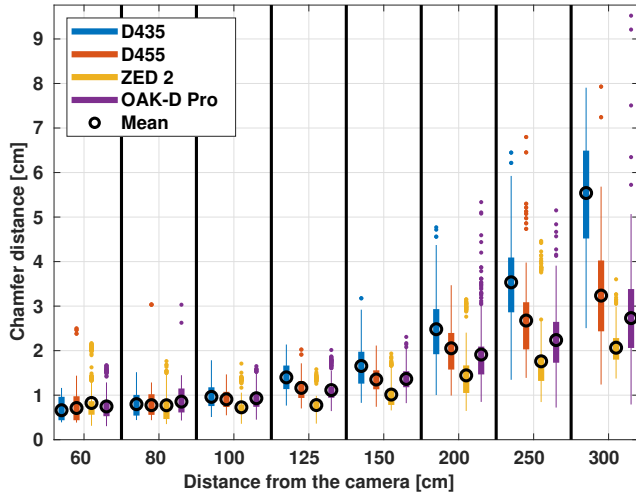


**FIGURE 13.** YCB objects perception – Chamfer Distance (CD). Bars show values from 25th to 75th percentile, whiskers represent non-outlier extreme points and dots represent outliers. Computed over 30 frames of 10 objects for each distance and camera. the lower the value, the better.

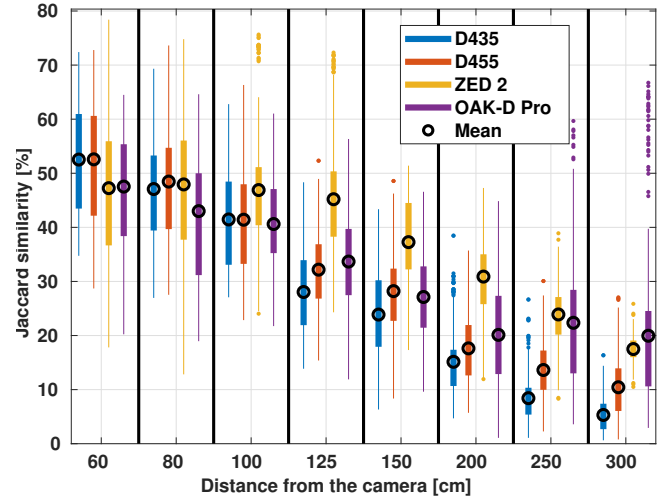


**FIGURE 15.** YCB objects perception – Jaccard Similarity (JS). Bars show values from 25th to 75th percentile, whiskers represent non-outlier extreme points and dots represent outliers. Computed over 30 frames of 10 objects for each distance and camera. The lower the value, the better.

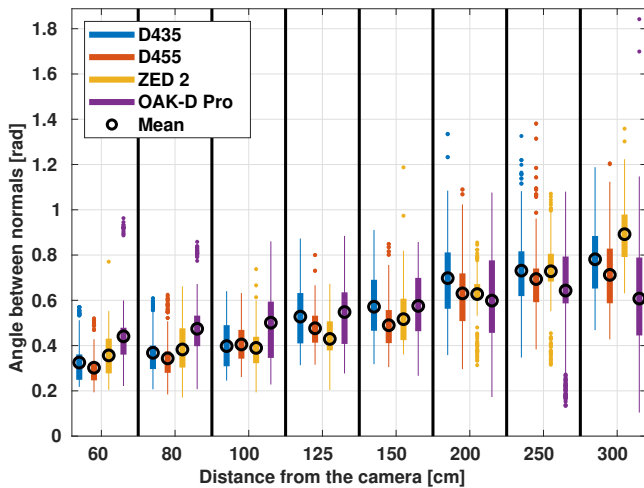


**FIGURE 14.** YCB objects perception – angles between the closest normals. Bars show values from 25th to 75th percentile, whiskers represent non-outlier extreme points and dots represent outliers. Computed over 30 frames of 10 objects for each distance and camera. The lower the value, the better.

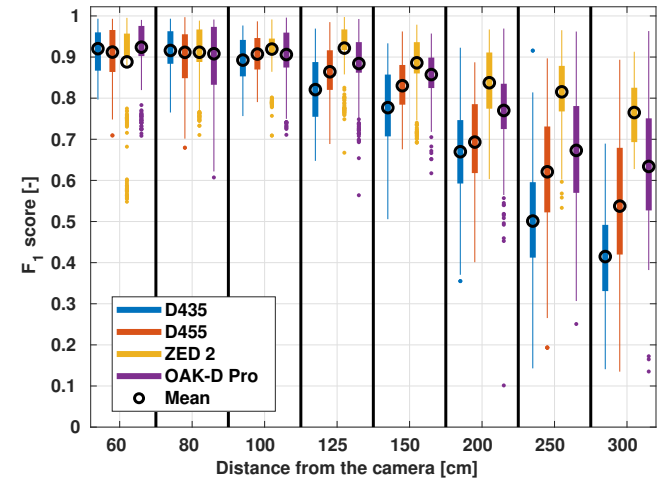


**FIGURE 16.** YCB objects perception –  $F_1$  score. Bars show values from 25th to 75th percentile, whiskers represent non-outlier extreme points and dots represent outliers. Computed over 30 frames of 10 objects for each distance and camera. The lower the value, the better.

a big difference between OAK-D Pro and the other cameras. Here, all cameras have similar results. It is again caused by the fact that some objects selected are flat, and therefore OAK-D Pro can estimate these well. However, the outliers (mainly at 60 cm) shows that it has problems with some objects.

Jaccard Similarity (JS) for this scenario is shown in Fig. 15. We can see that at lower distances, the RealSense devices perform the best and ZED 2 getting better with increasing distance. At higher distances, the mean is similar for both ZED 2 and OAK-D Pro, but based on the variance and outliers, ZED 2 performs comparably on all objects. OAK-D Pro, on the other hand, has many outliers—objects for

which the estimation is good, and thus the mean JS is higher. Analogous results are visible for the  $F_1$  score in Fig. 16. At lower distances, all cameras achieve similar scores, but gradually ZED 2 is the best with the highest  $F_1$  score and lower variance between objects.

Fig. 17 provides per-object comparison of CD. We provide only CD, but all graphs can be found, together with the data used to create these, at <https://osf.io/f2seb>. Generally, we can say that the most problematic objects are a *pitcher*, a *windex bottle*, a *football*, and a *drill*. The *windex bottle* is transparent, which is a challenging surface for feature matching. As the bottle was on the table, the cameras could see the table through it, which probably aided perception. If

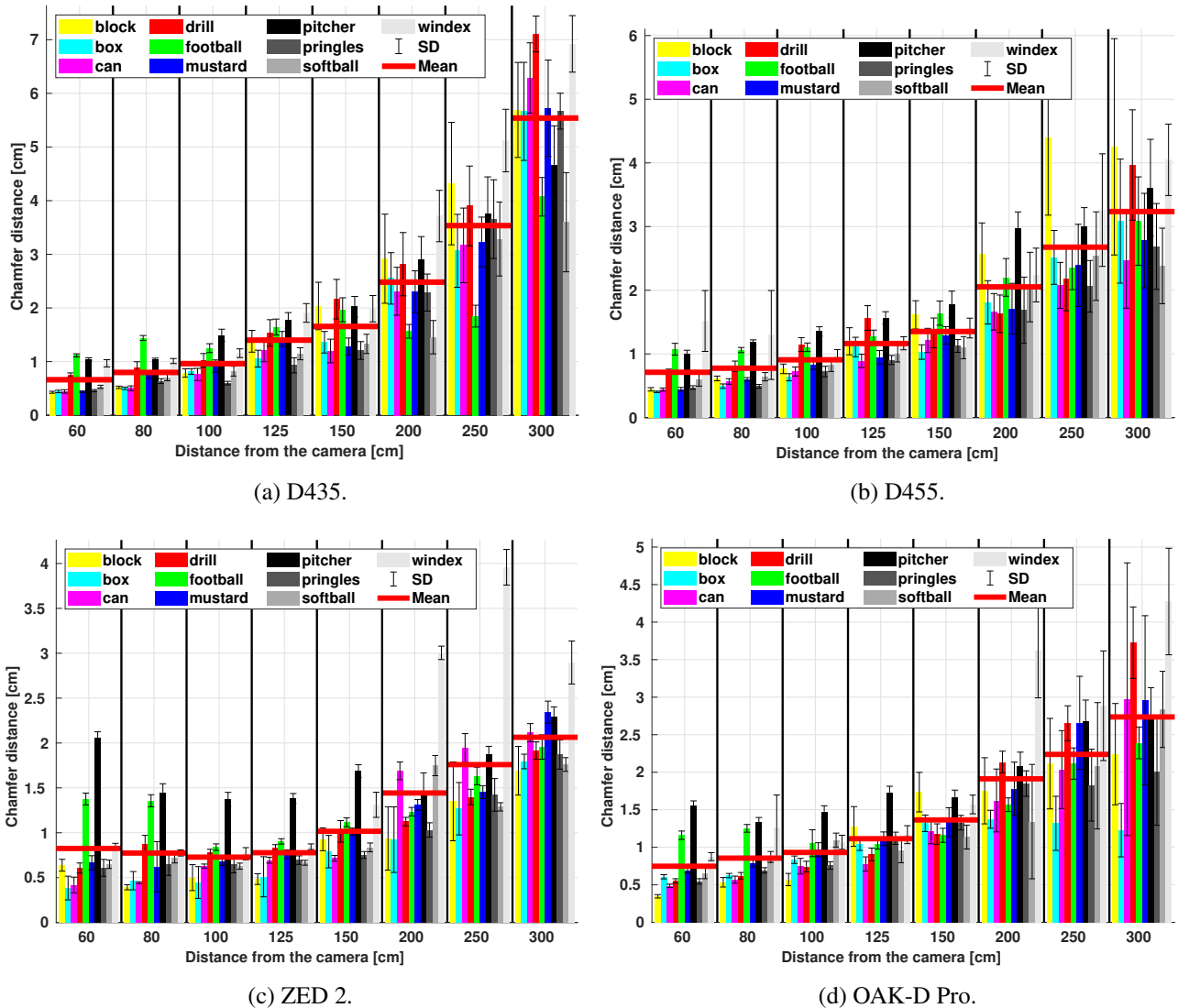


**FIGURE 17.** YCB objects perception – Chamfer Distance (CD) for individual objects. Red lines represent mean over all objects for a given distance. Computed over 30 frames for each distance.

there was nothing behind the bottle, the results would be even worse. The *drill* used has many small features on the surface that are hard to perceive, mainly at longer distances. In the case of *football* and *pitcher*, the main problem is probably the curvature—and, for the *pitcher*, the handle. We can see that the biggest error for these two have ZED 2 and OAK-D Pro. It supports the previous results and shows that these two cameras perform better with planar objects and suffer with more complex, curved objects.

**YCB objects perception – summary.** Overall, the results using YCB objects correspond to those using the plastic doll. All cameras are comparable up to 150 cm. After that, the best one is again ZED 2, now with OAK-D Pro being the second best. The reason why OAK-D Pro is not the worst as in the case of doll perception is that the dataset used contains some flat objects that are estimated correctly and decrease the

overall error over all the objects.

## V. CONCLUSION AND DISCUSSION

We compared four state-of-the-art stereoscopic depth cameras on more than 3,000 frames taken with each camera. The segmented data are available at <https://osf.io/f2seb>. Using six metrics, we compared the cameras on planar surface perception, plastic doll perception and on 10 household objects from the YCB dataset. The results show that even though the working principles are similar, individual cameras have different performance in different contexts and at different distances. In conclusion, on the basis of the results, we recommend the following. If your application requires an easy-to-setup and robust solution for lower distances (up to 90-100 cm) and is more object perception focused with unknown objects of arbitrary shapes, then the choice is RealSense D435. If

you want to work at higher distances or also be able to detect planar surfaces properly (e.g., in mobile robots and for SLAM), select RealSense 455 or Stereolabs ZED 2. Here, the choice depends on whether you can afford to have a dedicated GPU for depth estimation (ZED 2) or not (D455). If you want to detect planar surfaces and/or objects that are less complex (e.g., boxes) the choice would be ZED 2 or Luxonis OAK-D Pro—again depending on whether you have a GPU (then choose ZED 2) or not (choose OAK-D Pro). In case you also require AI features, you can choose ZED 2 or OAK-D Pro. The choice here is based on whether you want to compute the AI on-board (OAK-D Pro) or have a dedicated computer GPU (ZED 2).

The overall best camera is StereoLabs ZED 2. This camera provided the best results for planar surface estimation in terms of bias and standard deviation. Also, visually the point clouds created are the most flat. For plastic doll and YCB object perception, the camera also showed superior performance. For all metrics it achieved the best mean performance, while keeping the deviation between individual frames lower than the other cameras. It also provides easily accessible AI features like keypoint detection or face tracking. On the other hand, the camera requires CUDA-enabled GPU, which may be a drawback for some applications. ZED 2 also has a long baseline (the distance between two sensors in the physical camera) and works better from distances about 100 cm, which could be impractical for in some tasks like manipulation. On lower distances it tends to create holes in the object and miss some more complicated parts. From a user point of view, the API and associated software is not as intuitive as for Intel RealSense devices. At first, we had some problems setting the environment and installing the proper versions of the required libraries, which was never the case for RealSense cameras.

The other cameras have a more specific use case. The Luxonis OAK-D Pro camera provides on-board AI features without the need for an external GPU. It works great for planar surface, where it provides performance comparable with ZED 2 camera, while computing everything on-board. However, its performance decreases a lot when perceiving more complex objects. The camera basically groups points in layers of constant depths. At lower distances, the layers are close to each other, so the overall perceived shape is correct. At higher distances, the layers are far from each other—see Fig. 5, Fig. 7, and Fig. 12. In addition, the camera seems to “load” when started, i.e., sometimes first frames after the start tend to be unfocused and more noisy. The API and software are the least intuitive of all the cameras.

The RealSense D435 and D455 are the most typical RGB-D cameras currently used in robotics. They work on the same stereoscopic principle with IR projection computing everything on-board CPU without any additional AI features. The difference in these is the baseline that results in different performance. The D435 is smaller and therefore works at lower distances. The ideal range is only up to 3 m, so the performance decreases quickly with increasing distance, but up to 100 cm, the planar estimation is on par with other

cameras (except for ZED 2, which is better) and for shape estimation it is overall the best in this range. The D455 seems to work better on the plane estimation task and works better for bigger distances. The RealSense API and all other software is the best among all the cameras. However, we also encountered some problems. Sometimes, the cameras would not start properly without removing and reinserting the USB cable. Also, mainly D455 seems to have a fixed order of turning on RGB and depth channels. If it is done in incorrect order, the depth and RGB images are not correctly matched. D455 also has a low RGB resolution (1280x800), which can be, mainly together with high FOV, a problem for RGB-based computer vision applications such as keypoint detection.

Future work should also focus on comparing Time-of-Flight (ToF) sensors. Moreover, the cameras used are the state of the art in the time of publication, but the field is evolving rapidly, and it will be necessary to provide new studies when new sensors become available.

## REFERENCES

- [1] Depth Camera D435. <https://www.intelrealsense.com/depth-camera-d435/>.
- [2] Depth Camera D455 – Intel® RealSense™ Depth and Tracking Cameras. <https://www.intelrealsense.com/depth-camera-d455/>.
- [3] ZED 2i - Industrial AI Stereo Camera. <https://www.stereolabs.com/zed-2i/>.
- [4] OAK-D Pro. <https://docs.luxonis.com/hardware/products/OAK-D%20Pro>.
- [5] Marc-Antoine Drouin and Lama Seoud. Consumer-Grade RGB-D Cameras. In *3D Imaging, Analysis and Applications*, pages 215–264. Springer International Publishing, Cham, 2020.
- [6] Michael Riis Andersen, Thomas Jensen, Pavel Lisouski, Anders Krogh Mortensen, Mikkel Kragh Hansen, Torben Gregersen, and PIAU Ahrendt. Kinect Depth Sensor Evaluation for Computer Vision Applications. *Aarhus University*, pages 1–37, 2012.
- [7] Chuong V. Nguyen, Shahram Izadi, and David Lovell. Modeling Kinect Sensor Noise for Improved 3D Reconstruction and Tracking. In *2012 Second International Conference on 3D Imaging, Modeling, Processing, Visualization & Transmission*, pages 524–530, 2012.
- [8] Monica Carfagni, Rocco Furferi, Lapo Governi, Michaela Servi, Francesca Uccheddu, and Yary Volpe. On the Performance of the Intel SR300 Depth Camera: Metrological and Critical Characterization. *IEEE Sensors Journal*, 17(14):4508–4519, July 2017.
- [9] Francisco Lourenço and Helder Araújo. Intel RealSense SR305, D415 and L515: Experimental Evaluation and Comparison of Depth Estimation. In *Proceedings of the 16th International Joint Conference on Computer Vision, Imaging and Computer Graphics Theory and Applications*, pages 362–369. SCITEPRESS - Science and Technology Publications, 2021.
- [10] Alvaro Lopez Paredes, Qiang Song, and Miguel Heredia Conde. Performance Evaluation of State-of-the-Art High-Resolution Time-of-Flight Cameras. *IEEE Sensors Journal*, 23(12):13711–13727, June 2023.
- [11] Vladimir Tadic, Attila Toth, Zoltan Vizvari, Mihaly Klincsik, Zoltan Sari, Peter Sarcevic, Jozsef Sarosi, and Istvan Biro. Perspectives of RealSense and ZED Depth Sensors for Robotic Vision Applications. *Machines*, 10(3):183, March 2022.
- [12] Ahmed Abdelsalam, Mostafa Mansour, Jari Porras, and Ari Happonen. Depth Accuracy Analysis of the ZED 2i Stereo Camera in an Indoor Environment. *Robotics and Autonomous Systems*, 179:104753, September 2024.
- [13] Georg Halmetschlager-Funek, Markus Suchi, Martin Kampel, and Markus Vincze. An Empirical Evaluation of Ten Depth Cameras: Bias, Precision, Lateral Noise, Different Lighting Conditions and Materials, and Multiple Sensor Setups in Indoor Environments. *IEEE Robotics & Automation Magazine*, 26(1):67–77, March 2019.
- [14] Joana Dias, Pedro Simões, Nuno Soares, Carlos M. Costa, Marcelo R. Petry, Germano Veiga, and Luís F. Rocha. Comparison of 3D Sensors for Automating Bolt-Tightening Operations in the Automotive Industry. *Sensors*, 23(9):4310, January 2023.

- [15] Longsheng Fu, Fangfang Gao, Jingzhu Wu, Rui Li, Manoj Karkee, and Qin Zhang. Application of Consumer RGB-D Cameras for Fruit Detection and Localization in Field: A Critical Review. *Computers and Electronics in Agriculture*, 177:105687, October 2020.
- [16] Chiranjivi Neupane, Anand Koirala, Zhenglin Wang, and Kerry Brian Walsh. Evaluation of Depth Cameras for Use in Fruit Localization and Sizing: Finding a Successor to Kinect v2. *Agronomy*, 11(9):1780, September 2021.
- [17] Hui Chen and Wen Cui. A Comparative Analysis between Active Structured Light and Multi-View Stereo Vision Technique for 3D Reconstruction of Face Model Surface. *Optik*, 206:164190, March 2020.
- [18] Azmi Haider and Hagit Hel-Or. What Can We Learn from Depth Camera Sensor Noise? *Sensors*, 22(14):5448, January 2022.
- [19] Michel Heinemann, Jonas Herzfeld, Martin Sliwinski, Johannes Hinckeldeyn, and Jochen Kreuzfeldt. A Metrological and Application-Related Comparison of Six Consumer Grade Stereo Depth Cameras for the Use in Robotics. In *2022 IEEE International Symposium on Robot and Sensors Environments (ROSE)*, pages 01–07, November 2022.
- [20] Michaela Servi, Andrea Profili, Rocco Furferi, and Yary Volpe. Comparative Evaluation of Intel RealSense D415, D435i, D455, and Microsoft Azure Kinect DK Sensors for 3D Vision Applications. *IEEE Access*, 12:111311–111321, 2024.
- [21] Berk Calli, Arjun Singh, Aaron Walsman, Siddhartha Srinivasa, Pieter Abbeel, and Aaron M. Dollar. The YCB object and Model set: Towards common benchmarks for manipulation research. In *2015 International Conference on Advanced Robotics (ICAR)*, pages 510–517, 2015.
- [22] P.J. Besl and Neil D. McKay. A Method for Registration of 3-D Shapes. *IEEE Transactions on Pattern Analysis and Machine Intelligence*, 14(2):239–256, 1992.
- [23] Carsten Griwodz, Simone Gasparini, Lilian Calvet, Pierre Gurdjos, Fabien Castan, Benoit Maujean, Gregoire De Lillo, and Yann Lanthony. Alicevision Meshroom: An open-source 3D reconstruction pipeline. In *Proceedings of the 12th ACM Multimedia Systems Conference - MMSys '21*. ACM Press, 2021.
- [24] Clement Fuji Tsang, Maria Shugrina, Jean Francois Lafleche, Or Perel, Charles Loop, Towaki Takikawa, Vismay Modi, Alexander Zook, Jiehan Wang, Wenzheng Chen, Tianchang Shen, Jun Gao, Krishna Murthy Jatavallabhula, Edward Smith, Artem Rozantsev, Sanja Fidler, Gavriel State, Jason Gorski, Tommy Xiang, Jianing Li, Michael Li, and Rev Lebareddan. Kaolin: A Pytorch Library for Accelerating 3D Deep Learning Research.



**MATEJ HOFFMANN** (Senior Member, IEEE) received the Ph.D. degree in informatics from Artificial Intelligence Lab, University of Zurich, Zurich, Switzerland, in 2012.

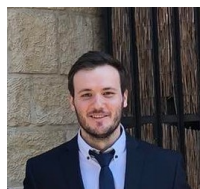
From 2013 to 2016, he conducted postdoctoral research with the iCub Facility of the Italian Institute of Technology, Genoa, Italy, supported by a Marie Curie Intra-European Fellowship. In 2017, he joined the Department of Cybernetics, Faculty of Electrical Engineering, Czech Technical University in Prague, where he is currently an Associate Professor and the Coordinator of the Humanoid and Cognitive Robotics Group. His research interests include humanoid, cognitive developmental, and collaborative robotics, as well as active perception for robot manipulation and grasping.

...

**LUKAS RUSTLER** received his BSc. and MSc. degrees in Cybernetics and Robotics from the Faculty of Electrical Engineering, Czech Technical University in Prague in 2019 and 2022, respectively.

He is a doctoral student at the Humanoid and Cognitive Robotics Group (Faculty of Electrical Engineering, Czech Technical University in Prague) under the supervision of Matej Hoffmann.

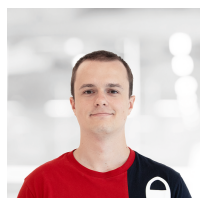
His research interests include robot kinematic cal-



ibration, physical human-robot interaction, grasping, and active multi-modal perception.

**VOJTECH VOLPRECHT** received his BSc. and MSc. degrees in Artificial Intelligence from the Faculty of Electrical Engineering, Czech Technical University in Prague in 2022 and 2024, respectively.

He is currently working as a researcher and software developer in the medical company BTL Medical Technologies. His research interests include planning in robotics, perception and estimation from RGB-D data and artificial intelligence in



medicine.